Fault-Adaptive Traffic Density Estimation for the Asymmetric Cell Transmission Model

Stelios Timotheou, Christos G. Panayiotou and Marios M. Polycarpou

Abstract— **The often faulty nature of measurement sensors hinders reliable traffic state estimation, affecting in this way various transportation operations such as traffic control and in-car navigation. This work proposes a systematic, model-based, online and network-wide approach to achieve robust and good quality state estimation in the presence of sensor faults. The approach is comprised of three stages aiming at 1) identifying the level of faulty behavior of each sensor using a novel fault-tolerant optimization algorithm, 2) isolating faults, and 3) improving state estimation performance by adaptively compensating sensor faults and resolving the state estimation problem. The approach is examined in the context of the Asymmetric Cell Transmission Model for freeway traffic density estimation. Simulation results demonstrate the effectiveness of the proposed fault-adaptive approach, yielding estimation performance very close to the one obtained with healthy measurements, irrespective of the fault magnitude and type.**

I. INTRODUCTION

Traffic state estimation (TSE) is an important topic in transportation engineering that enables a wealth of applications related to the monitoring and control of intelligent transportation systems (ITS) [1]. However, TSE is a challenging task for several reasons. Firstly, the large-scale nature of the transportation network makes the solution of the TSE problem difficult for city-size networks, while a large portion of the transportation network remains unmonitored. In addition, there are several heterogeneous sources that need to be fused together to improve TSE, with each measuring different traffic parameters and having distinct features. Furthermore, the unpredictable nature of human driving behavior results in large modeling uncertainties. Finally, an important challenge often neglected is associated with the presence of faulty sensors that provide erroneous measurements, significantly deteriorating the estimation performance. Fault-tolerant and fault-adaptive TSE is the main focus of this paper.

The main approaches for TSE are *model-based*, making use of traffic flow physics to construct appropriate models and efficiently incorporate traffic data to obtain estimation and/or prediction of traffic. The most common approaches utilizes first or second order density-flow or velocity models, combined with different Kalman-filtering approaches (linear [2], extended [3], ensemble [4]) to optimize estimation performance in the presence of noise. In the context of the Asymmetric Cell Transmission Model (ACTM), TSE has also been examined from a Kalman filtering perspective in [5], [6]. These works develop implicit mode switching methods to alternate between cell congestion modes and apply Kalman filtering in the resulting linear time-variant system.

Despite the large body of literature on TSE, most research works assume non-faulty traffic sensors, an assumption that in practice is not true. For example, approximately 90% of the traffic sensors in California are Inductive Loop Detectors (ILDs) which are quite unreliable. In fact, it has been reported that only 60% of these sensors provide reliable measurements on a typical day [7]. In addition, existing research on faulty traffic sensors typically considers separately the issues of fault detection, fault correction and state estimation. Most approaches for fault detection consider certain statistical or probabilistic measures (e.g. number of samples in a day with non-zero occupancy and zero flow, probability of counting a certain number of vehicles) and report faults when measured values are below/above a certain threshold defined according to physical limits or empirical data [8], [9]. Other approaches compare measurements with other highly correlated measurements to detect faults (e.g. from neighboring sensors [10] and historical data [11]). The aforementioned fault detection techniques for traffic sensors have several drawbacks; statistical and probabilistic threshold-based measures need to be considered for a large horizon (up to 1 day) to provide good results and hence are not suitable for real-time fault detection and also cannot detect temporal ILD failures, while comparison-based methods can exhibit multiple false positive alarms due to alternating traffic patterns. Correction methods are based mostly on linear interpolation or moving window averaging over time and space [12] but do not consider the overall network dynamics to capture traffic transitions between links.

In this work we examine TSE in the presence of faulty sensors and develop a model-based fault-adaptive approach that achieves system-wide robust and good quality TSE. The proposed approach is composed of three stages. In the first stage a novel optimization problem for fault-tolerant moving horizon estimation is solved to identify the level of faulty behavior of each sensor. In the second stage each sensor is marked as faulty or non-faulty, while in the third stage a second optimization problem is solved to improve the accuracy of the state estimation based on the identification of faulty sensors. The approach is examined in the context of ACTM for freeway traffic density estimation.

The remainder of this paper is organized as follows.

This work is partially funded by the European Research Council Advanced Grant FAULT-ADAPTIVE (ERC-2011-AdG-291508).

The authors are with the KIOS Research Center for Intelligent Systems and Networks, University of Cyprus {timotheou.stelios, christosp, mpolycar}@ucy.ac.cy.

Section II provides some preliminary results on state estimation of dynamical systems that will be utilized for the developed approach. Section III describes the ACTM that is used to model the traffic dynamics, while Section IV briefly outlines the TSE problem and introduces the developed fault-tolerant estimation method. Section V exploits the developed fault-tolerant approach to further improve estimation quality through a fault-adaptive procedure. Section VI demonstrates the performance of the proposed TSE approaches, while Section VII concludes the paper.

Notation: All boldface letters indicate vectors (lower case) or matrices (upper case), while calligraphic letters denote sets. The superscripts $(\cdot)^T$ and $(\cdot)^{-1}$, denote the transpose and the matrix inverse respectively. $\|\mathbf{x}\|^2_{\mathbf{T}} = \mathbf{x}^T\mathbf{T}\mathbf{x}$ denotes the Euclidean weighted norm of a vector $\mathbf{x}$. $\mathbf{X}_{M_1}^{M_2}$ denotes a matrix defined as $\mathbf{X}_{M_1}^{M_2} = [\mathbf{x}_{M_1}, ..., \mathbf{x}_{M_2}]$, where $\mathbf{x}_i$ is a column vector. $\mathbf{1}\{z\}$ is an indicator function which is equal to 1 if z is true and 0 otherwise. $\|\mathbf{x}\|_0 = \sum_i 1\{x_i \neq 0\}$ and $\|\mathbf{x}\|_1 = \sum_i |x_i|$ denote the l_0 and l_1 norms, respectively.

II. Moving Horizon Estimation

In this section we discuss Moving Horizon Estimation [13] of linear time-variant dynamical systems that are important for the developed TSE approaches.

Consider the following discrete, stochastic, linear, time-variant, dynamical system with state vector $\mathbf{x}_k \in \mathbb{R}^{N\times 1}$, input $\mathbf{u}_k \in \mathbb{R}^{N\times 1}$ and noisy observations $\mathbf{z}_k \in \mathbb{R}^{M\times 1}$ [14]

$$\mathbf{x}_k = \mathbf{A}_{k-1}\mathbf{x}_{k-1} + \mathbf{B}_{k-1}\mathbf{u}_{k-1} + \mathbf{w}_{k-1}, \quad (1)$$

$$\mathbf{z}_k = \mathbf{H}_k\mathbf{x}_k + \mathbf{v}_k, \quad (2)$$

where $\mathbf{x}_0$, $\mathbf{w}_k$, $\mathbf{v}_k$ are the random initial state, the process noise and the measurement noise vectors, respectively. These components are assumed to be zero-mean, uncorrelated Gaussian random vectors with covariance $\mathbf{P}_0$, $\mathbf{Q}_k$ and $\mathbf{R}_k$.

The *state estimation* or *filtering problem* aims to find the best approximation of the state-vector $\hat{\mathbf{x}}_K$ given the set of the first K observations, $\mathbf{Z}_1^K = \{\mathbf{z}_k,\, k = 1, ..., K\}$ and input vectors $\mathbf{U}_0^{K-1} = \{\mathbf{u}_k,\, k = 0, ..., K-1\}$. For this class of dynamical systems, the optimal estimation of the state-vector $\hat{\mathbf{x}}_K$ is given by the Kalman Filter (KF) following a two-step recursive procedure for $k = 1, ..., K$ to produce a statistically optimal system state; for details see [15].

The same result with KF can be obtained by considering a maximum *a posteriori* formulation for the problem of estimating state $\hat{\mathbf{x}}_K$, given by [13]:

$$\min_{\mathbf{X}} \Phi_1^K(\mathbf{X}_1^K) + \frac{1}{2}\mathbf{x}_0^T\mathbf{P}_0^{-1}\mathbf{x}_0 \quad (3)$$

$$\Phi_{M_1}^{M_2}(\mathbf{X}_{M_1}^{M_2}) = \frac{1}{2}\sum_{k=M_1}^{M_2}\Big\{\|\mathbf{z}_k - \mathbf{H}_k\mathbf{x}_k\|^2_{\mathbf{R}_k^{-1}} + \|\mathbf{x}_k - \mathbf{A}_{k-1}\mathbf{x}_{k-1} - \mathbf{B}_{k-1}\mathbf{u}_{k-1}\|^2_{\mathbf{Q}_{k-1}^{-1}}\Big\} \quad (4)$$

Formulation (3) is a least squares problem that can be solved analytically in $O(N^3K^3)$ as a linear $NK \times NK$ system of equations, or in $O(N^3K)$ if the special block tri-diagonal structure of the system is exploited [16].

To reduce the computational complexity of increasing K, an MHE approach considers a moving window backwards in time of length W, i.e.,

$$\min_{\mathbf{X}} \Phi_{K-W+1}^K(\mathbf{X}_{K-W+1}^K) + \Gamma_{K-W}(\mathbf{x}_{K-W}), \quad (5)$$

where $\Gamma_{K-W}(\mathbf{x}_{K-W})$ is the *arrival cost* (AC) summarizing the effect of the discarded data on the current states and obtained through partial minimization with respect to decision variables $\mathbf{x}_0$, $\mathbf{x}_1$,...,$\mathbf{x}_{K-W-1}$ [17],

$$\Gamma_{K-W}(\mathbf{x}_{K-W}) = \min_{\mathbf{x}_0,\ldots,\mathbf{x}_{K-W-1},} \Phi_1^{K-W}(\mathbf{X}_1^{K-W}) + \mathbf{x}_0^T\mathbf{P}_0^{-1}\mathbf{x}_0. \quad (6)$$

In general, it is difficult to obtain the AC when having nonlinear model dynamics or additional constraints leading to the development of approximation methods (e.g. [17]). However, under a linear model with Gaussian noise and no constraints the AC attains the closed form

$$\Gamma_{K-W}(\mathbf{x}) = (\mathbf{x} - \hat{\mathbf{x}}_{K-W})^T\mathbf{P}_{K-W}^{-1}(\mathbf{x} - \hat{\mathbf{x}}_{K-W}) \quad (7)$$

where $\mathbf{P}_{K-W}$ and $\hat{\mathbf{x}}_{K-W}$ result from the $(K-W)$-th step of KF [14].

Although the MHE approach is still computationally more demanding compared to the Kalman filter ($O(N^3W)$ compared to $O(N^3)$), its main advantage is that it can easily incorporate model-related constraints. Such constraints include physical model limitations, e.g. lower and upper bounds on the state variables, or artificially added constraints that aim to capture some insights regarding the dynamics such as state transition smoothness or sparse state changes [16], [17]. In this work we exploit the MHE approach to incorporate additional constraints that provide fault-tolerance in the presence of sensor faults.

III. Asymmetric cell transmission model

The cell transmission model (CTM) is employed to describe the traffic dynamics due to its simplicity, popularity and ability to model different boundary phenomena. CTM is a first-order macroscopic traffic flow model which is based on a trapezoidal flow-density fundamental diagram and is characterized by the macroscopic parameters u^f, Q^M, w and ρ^J. The free-flow speed, u^f (km/h), is the average speed at which vehicles travel in a road when it is empty. The capacity of the road Q^M (veh/h) is the maximum flow rate of vehicles through the road. The backward wave propagation speed w is the average speed at which a vehicle queue propagates upstream within a highly congested region. The jam density ρ^J is the maximum density of vehicles that can be reached within the road under congestion conditions. In addition, critical densities $\rho^{C1} = Q^M/u^f$ and $\rho^{C2} = \rho^J - Q^M/w$ separate the three regions of cell i: a) free-flow region ($0 \leq \rho \leq \rho^{C1}$), b) maximum capacity region ($\rho^{C1} \leq \rho \leq \rho^{C2}$), and (c) congestion region ($\rho^{C2} \leq \rho \leq \rho^J$), respectively. In the CTM both time and space are discrete. Time is partitioned into time-steps T_s, while each road segment is divided into homogeneous sections called *cells* of equal length in a way that one vehicle takes one time-unit to travel through one cell at free-flow speed.

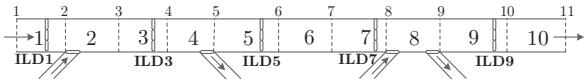

Fig. 1: Example of ACTM for a freeway segment with two on-ramp and two off-ramps.

In this work a generalization of CTM is considered, called the asymmetric CTM (ACTM) which allows for non-homogeneous cells, with cell $i \in \mathcal{N} = \{1, ..., N\}$ having length L_i, such that, $L_i \geq u^f T_s$. In ACTM the traffic density of cell i at time unit t, $\rho_{i,t}$, evolves according to [18]

$$\rho_{i,t+1} = \rho_{i,t} + (T_s/L_i)(q_{i,t}^{in} - q_{i,t}^{out}), \tag{8}$$

where $q_{i,t}^{in}$ and $q_{i,t}^{out}$ (veh/h) denote the inflow and outflow of vehicles of cell i during $[tT_s, (t+1)T_s)$. The dynamics of parameters $q_{i,t}^{in}$ and $q_{i,t}^{out}$ are determined from the conditions on the boundary between consecutive cells. In this work, five different sets of inter-cell connections are considered (simple, input, output, merge and diverge) to model a freeway stretch, where connection i models the boundary between cells $i-1$ and i.

IV. Fault-Tolerant Traffic state estimation

Traffic state estimation refers to the process of estimating the true values of variables that define the state from measurements of traffic characteristics (e.g., occupancy, counts, speeds). This need emanates from two important measurement weakness: a) low-quality due to noise, faults and synchronization errors and b) local nature in both space (collected at a point or a short road section) and time (moving observers collect a single measurement at different locations). In the context of ACTM, to have full knowledge of the system state (density, speed and flow), it is sufficient to estimate the traffic density $\boldsymbol{\rho}_t = [\rho_{1,t}, \rho_{2,t}, ..., \rho_{N,t}]^T$, at every cell and time step; the flow can then be obtained from the flow-density fundamental diagram and the speed from the relationship *flow=density×speed*. For the traffic density dynamics of ACTM we consider the following process/measurement model based on (8)

$$\boldsymbol{\rho}_{t+1} = \boldsymbol{\rho}_t + (T_s/L_i)(\mathbf{q}_t^{in} - \mathbf{q}_t^{out}) + \mathbf{w}_t, \tag{9}$$

$$\mathbf{z}_t = \min\left\{\boldsymbol{\rho}^J, \max\left\{\mathbf{0}, \boldsymbol{\rho}_t + \mathbf{v}_t\right\}\right\}, \tag{10}$$

where the random components $\boldsymbol{\rho}_0$, $\mathbf{w}_t$, $\mathbf{v}_t$ are zero mean, uncorrelated Gaussian random vectors with covariance $\mathbf{P}_0$, $\mathbf{Q}_t$, $\mathbf{R}_t$, respectively. Here, we have assumed for simplicity that measurements of traffic density, $z_{i,t}$, are available from ILD sensors, $i \in \mathcal{M}$ at time-step t, where $\mathcal{M}$ is the set of sensors, and that the process and measurement models are updated with the same frequency. For simplicity and without loss of generality it is further assumed that the on-ramp inputs and off-ramp split ratios are known.

Since parameters $\mathbf{q}_t^{out}$ and $\mathbf{q}_t^{in}$ are piecewise linear, the traffic density dynamics in (9) are also piecewise linear (for details see [5]). To deal with this issue we adopt the implicit mode switching approach [5], [6] which considers the estimation $\hat{\boldsymbol{\rho}}_t$, as an indication of the active linear segment (free-flow, maximum-capacity or congestion) of $\mathbf{q}_t^{out}$ and $\mathbf{q}_t^{in}$ of each cell connection for the period $[tT_s, (t+1)T_s)$. In this way, a time-variant linear model of the form (1)-(2) is constructed for the estimation of $\boldsymbol{\rho}_{t+1}$, whose parameters $\mathbf{A}_t$ and $\mathbf{b}_t$ result from the active linear segment of each inter-cell connection.

In the presence of faulty sensors a more appropriate measurement model is

$$\mathbf{z}_t = \min\left\{\boldsymbol{\rho}^J, \max\left\{\mathbf{0}, \boldsymbol{\rho}_t + \mathbf{v}_t + \mathbf{o}_t\right\}\right\}, \tag{11}$$

where $o_{i,t}$, is an unknown variable with value zero if sensor $i \in \mathcal{M}$ is not faulty at time t and non-zero otherwise. Correct recovery of both $\boldsymbol{\rho}_t$ and $\mathbf{o}_t$ estimates the state and identifies faulty measurements; nonetheless, this task is impossible as model (11) is unobservable. Capitalizing on the fact that $o_{i,t}$, is expected to be sparse, i.e. only a small number of elements will be non-zero, can yield suprisingly good estimation results [19]. If a specific number of bad data is expected, say n_f then the problem can be solved as

$$\min_{\mathbf{X},\mathbf{O}} \Psi_{K-W+1}^{K}(\mathbf{X}_{K-W+1}^{K}, \mathbf{O}_{K-W+1}^{K}) + \Gamma_{K-W}(\mathbf{x}_{K-W}) \tag{12}$$

$$\text{s.t.} \sum_{k=K-W+1}^{K} \|\mathbf{o}_k\|_0 \leq n_f, \tag{13}$$

where $\Psi_{M_1}^{M_2}(\bullet)$ and $\Gamma_{K-W}(\bullet)$ are given by (14) and (7).

$$\Psi_{M_1}^{M_2}(\mathbf{X}_{M_1}^{M_2}, \mathbf{O}_{M_1}^{M_2}) = \frac{1}{2}\sum_{k=M_1}^{M_2}\Big\{\|\mathbf{z}_k - \mathbf{H}_k\mathbf{x}_k - \mathbf{o}_k\|_{\mathbf{R}_k^{-1}}^2 + \|\mathbf{x}_k - \mathbf{A}_{k-1}\mathbf{x}_{k-1} - \mathbf{B}_{k-1}\mathbf{u}_{k-1}\|_{\mathbf{Q}_{k-1}^{-1}}^2\Big\}. \tag{14}$$

Due to the presence of the l_0-norm the problem is NP-hard and hence difficult to solve for large problems; one approach often taken is to convexify the problem by considering the l_1-norm, i.e. minimizing (12) subject to the constraint $\sum_k \|\mathbf{o}_k\|_1 \leq n_f$. Equivalently, the problem can be expressed in an unconstrained form as

$$\min_{\mathbf{X},\mathbf{O}} \Psi_{K-W+1}^{K}(\mathbf{X}_{K-W+1}^{K}, \mathbf{O}_{K-W+1}^{K}) + \Gamma_{K-W}(\mathbf{x}_{K-W}) + \lambda\sum_k \|\mathbf{o}_k\|_1 \tag{15}$$

where λ is a positive regularization parameter to trade-off between detecting faults and optimizing cost. The effectiveness of (15) is due to the fact that the $l1$-norm penalty term enforces sparsity in the number of non-zero $o_{i,k}$ elements which is expected to hold true if bad measurements are infrequent events. Nonetheless, as problem (15) identifies faults irrespective of the sensor and the time step it can perform well in the presence of random faults but not when faulty sensors exist for large time periods.

In this work, a different formulation is proposed that aims to achieve sensor fault-tolerance rather than measurement fault-tolerance. Towards this direction we define the *maximum fault residual*, $y_{i,t}$, of sensor i at time t as

$$y_{i,t} = \max_{k=t-W+1,...,t}\{|o_{i,k}|\} \tag{16}$$

which associates a value with sensor i equal to the maximum $o_{i,t}$ element for the moving window considered. This results in convex formulation (17)-(19).

$$\min_{\mathbf{X},\mathbf{O},\mathbf{y}} \ \Psi^{K}_{K-W+1}(\mathbf{X}^{K}_{K-W+1}, \mathbf{O}^{K}_{K-W+1}) + \Gamma_{K-W}(\mathbf{x}_{K-W}) + \lambda \sum_{i\in\mathcal{M}} y_{i,K} \quad (17)$$

$$\text{s.t. } o_{i,k} \leq y_{i,K},\ k = K-W+1, ..., K,\ i \in \mathcal{M}, \quad (18)$$

$$-o_{i,k} \leq y_{i,K},\ k = K-W+1, ..., K,\ i \in \mathcal{M}. \quad (19)$$

Formulation (17)-(19), guarantees satisfaction of equations (16) because constraints (18) and (19) are equivalent to $\max_{k=t-W+1,...,t} |o_{i,k}| \leq y_{i,K}$, while the penalty term $\lambda \sum_{i\in\mathcal{M}} y_{i,K}$ ensures that each $y_{i,K}$, $i \in \mathcal{M}$, will take the smallest possible value within the feasible set, yielding (16). The difference between formulations (15) and (17)-(19) is that the latter aims to minimize the maximum absolute error for each sensor over the moving horizon which means that the optimization problem will try to identify a few faulty sensors rather than try to compensate for bad measurements.

As we consider an MHE approach on a time-variant linear model, it is important to mention that once $\mathbf{A}_t$ and $\mathbf{b}_t$ are constructed based on $\hat{\boldsymbol{\rho}}_t$, constraints are added to ensure that the estimated $\hat{\mathbf{x}}_t$ in future time indices $k = t+1, ..., t+M$ remain within the initially identified region. Regarding the AC, we consider Eq. (7) as a good approximation of this term, as it is optimal for the error-free case.

V. Fault-Adaptive Traffic-State Estimation

Although formulation (17)-(19) achieves robust TSE in the presence of faulty sensors, it may reduce the quality of the TSE under healthy operating conditions. For this reason, this section proposes a fault-adaptive algorithm that aims to provide the best of both worlds (healthy versus faulty operation) by detecting faulty sensors and compensating only for their respective identified fault residuals. The procedure is outlined in Algorithm 1.

The first stage of the algorithm during time-step t involves the solution of problem (17)-(19) to obtain $y_{i,t}$ and $o_{i,k}$, $i \in \mathcal{M}$, $k = t-W+1, ..., t$, as the magnitude of these parameters is representative of potentially faulty sensors. In the second stage, a short-history C_w of measurements and maximum fault residuals are fed into Algorithm 2 to decide which are the healthy and which are the faulty sensors. In the third stage, the faulty sensor measurements are compensated according to the $o_{i,k}$ values obtained in stage 1, and the TSE problem is resolved, with no fault-tolerance consideration.

Algorithm 2 runs every time-step t to detect the currently faulty sensors given a short-history $C_w > W$ of values for parameters $y_{i,k}$ and $z_{i,k}$, $k \in \{t-C_w, ..., t-1, t\}$, for each sensor. This is achieved by separating the considered $y_{i,k}$ values into two clusters, identifying whether the clusters belong to same or different data class (healthy or faulty) and classifying the current time value $y_{i,t}$ appropriately. Towards this direction, lines 5-9 aim to provide an estimation of the average fluctuation of the maximum fault residuals due to the inherent noise. For this reason the moving average of

Algorithm 1 :Online Fault-Adaptive TSE

1: **for each** time-step t **do**
2: **Stage 1**: Solve problem (17)-(19) to obtain $y_{i,t}$ and $o_{i,k}$, $i \in \mathcal{M}$, $k = t-W+1, ..., t$.
3: **Stage 2**: Run Algorithm 2 to detect the set of faulty sensors, $\mathcal{F}_t$.
4: **Stage 3a**: Compute new measurement values for fault sensors $\hat{z}_{j,k} = z_{j,k} + o_{j,k}$, $j \in \mathcal{F}_t$, $k = t-W+1, ..., t$.
5: **Stage 3b**: Solve problem (5) using measurements $\hat{\mathbf{z}}_j$, $j \in \mathcal{F}_t$ and $\mathbf{z}_i$, $i \notin \mathcal{F}_t$ to obtain $\hat{\boldsymbol{\rho}}_t$.
6: **end for**

Algorithm 2 : Sensor Fault Detection

1: **Input**: $y_{i,k}$, $z_{i,k}$, $i \in \mathcal{M}$, $k \in \{t-C_w, ..., t-1, t\}$.
2: **Output**: $\mathcal{F}_t$
3: **Initialization**: $\mathcal{F}_t = \oslash$.
4: **for each** (sensor $i \in \mathcal{M}$) **do**
5: $\tilde{\mathbf{z}}_i = \text{movavg}(\mathbf{z}_i, W)$.
6: **for** ($k \in \{t-C_w, ..., t-1, t-W\}$) **do**
7: Set $\xi_{i,k} = |\max_{\tau=k,...,k+W}\{\tilde{z}_{i,\tau} - z_{i,\tau}\}|$
8: **end for**
9: Set $\mu_i^{\xi} = \text{mean}(\boldsymbol{\xi}_i)$.
10: $[\mathcal{T}_1, \mathcal{T}_2]$ = kmeans$(\mathbf{y}_i, 2)$.
11: Set $\mu_i^l = \underset{k\in\mathcal{T}_l}{\text{mean}}(y_{i,k})$, $\sigma_i^l = \underset{k\in\mathcal{T}_l}{\text{std}}(y_{i,k})$, $l = \{1, 2\}$.
12: **if** $(\mu_i^2 - 2\sigma_i^2 \geq \mu_i^1 + 2\sigma_i^1)\&(\mu_i^2 \geq \mu_i^{\xi})\&(t \in \mathcal{T}_2)$ **then**
13: $\mathcal{F}_t = \mathcal{F}_t \cup \{i\}$.
14: **else if** $(\mu_i^1 \geq \mu_i^{\xi})$ **then**
15: $\mathcal{F}_t = \mathcal{F}_t \cup \{i\}$.
16: **end if**
17: **end for**

the ith sensor's measurements is constructed (line 5), along with the values of the approximate maximum fault residuals in the absence of faults, $\xi_{i,k}$ (lines 6-8) and the approximate average fluctuation over the considered history, μ_i^{ξ} (line 9). In line 10, parameters $y_{i,k}$ of sensor i are clustered into two sets $\mathcal{T}_1$ and $\mathcal{T}_2$ that hold the time-indices (k) of $y_{i,k}$ using *kmeans* algorithm; without loss of generallity it is assumed that the average maximum fault residual of the second cluster, μ_i^2, is larger than that of the first cluster, μ_i^1. Upon clustering the data there are three cases to consider: (I) $\mathcal{T}_1$ and $\mathcal{T}_2$ represent healthy and faulty data respectively, (II) both $\mathcal{T}_1$ and $\mathcal{T}_2$ represent faulty data, and (III) both $\mathcal{T}_1$ and $\mathcal{T}_2$ represent healthy data. Case I is true if there is clear separation between the data of the two clusters (line 12); in this case, sensor i is classified as faulty for time-step t if $y_{i,t}$ belongs to the second cluster, i.e. $t \in \mathcal{T}_2$ (lines 12-13). A sensor is also classified as faulty when both clusters represent faulty data (case II); this is true when both μ_i^1 and $\mu_i^2 \geq \mu_i^1$ are larger than μ_i^{ξ} (lines 14-15).

VI. Simulation results

To evaluate the performance of the proposed algorithms we consider a 3-lane freeway stretch of 10 cells with lengths $L_i = \{0.5, 0.6, 0.5, 0.5, 0.75, 0.6, 0.5, 0.5, 0.8, 0.75\}$km, as

shown in Fig. 1. Traffic enters the freeway from the mainline input as well as from on-ramps in cells 2 and 8 following a typical morning traffic pattern and maximum values 4500 veh/h, 750 veh/h, and 600 veh/h, respectively, and exits from the mainline output and off-ramps on cells 4 and 8 with split ratios in the range [0.15, 0.2]. We consider the following ACTM parameter values: $u^f = 100$km/h, $T_s = 10$s, $w = 30$km/h, $Q^M = 6000$veh/h, $\rho^J = 300$veh/km; the simulation time is considered to be 3h. For simplicity we assume that the model and measurement noise are independent zero-mean Gaussian random processes for all sensors. The performance of three algorithms is examined:

1) **KF**: Kalman Filtering.
2) **FTS**: Formulation (17)-(19) which provides fault-tolerance against sensor faults.
3) **FAS**: Algorithm 1 which provides fault-adaptive TSE in the presence of sensor faults.

For FTS algorithm, parameters λ and W are set to values 1.4 and 10 which have been experimentally observed to perform well, while for Algorithm 2 parameter C_w is set to 90 (15mins).

Fig. 2 examines the TSE mean square error (MSE) performance of algorithms KF, FTS and FAS for varying value of one multiplicative fault at sensor ILD3 during period [0.5h,1.5h], for different measurement and process noise covariance values. The figures illustrate that both approaches provide robust TSE for all scenarios considered with almost constant behavior irrespective of the fault magnitude. Another interesting observation is that the relative performance of FTS and FAS depends on the relationship of the measurement and process noise. For equal process and measurement noise variance both approaches perform equally well, FTS is slightly better than FAS when the measurement noise variance is large than the process noise variance, while FAS is the clear winner when the process noise variance is larger than the measurement noise variance, achieving two times the performance of FTS. Notice also that FAS achieves performance almost equal to the case with no sensor faults for all scenarios considered[1]. Similar behaviour is observed for an additive sensor fault at ILD3 of varying magnitude[2].

The same simulation setup is also used to examine the effectiveness of the sensor fault detection algorithm (Algorithm 2). For this reason we have adopted the Fault Detection Accuracy criterion defined as the percentage of true positives (correctly classified faulty sensors) and true negatives (correctly classified healthy sensors) over the total number of fault detection decisions. Fig. 3 depicts the fault detection accuracy for different noise scenarios and varying additive and multiplicative fault magnitude. The accuracy of our detection algorithm exceeds 94% in all cases examined except from additive/multiplicative fault value equal to 5/1.1 when $\mathbf{R} = \mathbf{I}$ and $\mathbf{Q} = 9\mathbf{I}$. The main reason for the low

[1]In Figs. 2 and 3, an additive fault of value 0 and a multiplicative fault of value 1 represent the non-faulty case.

[2]Let $\rho_{i,t}$ be the true traffic density at sensor i. A *multiplicative sensor fault* of value α results in measurement $z_{i,t} = \alpha(\rho_{i,t} + v_{i,t})$. An *additive sensor fault* of value β results in measurement $z_{i,t} = \beta + \rho_{i,t} + v_{i,t}$.

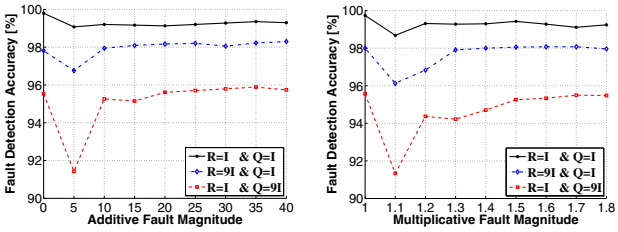

(a) (b)

Fig. 3: Fault detection accuracy for different measurement and process noise scenarios and varying (a) additive, and (b) multiplicative fault magnitude at ILD3.

accuracy in this case is the large measurement fluctuation that makes a small fault indistinguishable from noise. In this case, the good news is that the main factor deteriorating the TSE quality is due to the noise variance rather than the fault itself, so that the overall TSE performance is similar to the non-faulty case.

The ability of FTS to identify multiple combinations of faults is illustrated in Fig. 4 which depicts more closely faulty scenarios with up to two faults for all combinations of ILDs. For this purpose, two overlapping faults are considered, one multiplicative with value 1.5 for period $[0.5h, 1.5h]$ and one additive of magnitude 10 for period $[1.0h, 2.5h]$, while measurement and process noise variance are set to $\mathbf{R} = \mathbf{I}$ and $\mathbf{Q} = \mathbf{I}$, respectively. As can been observed, FTS successfully identifies the faults through the maximum fault residual values in all scenarios considered; this observation holds true even for the overlapping period of the two faults [1.0h, 1.5h].

VII. Conclusions and Future Work

This paper has investigated fault-tolerant and fault-adaptive traffic state estimation. Towards this direction a fault-tolerant model-based moving horizon estimation approach has been developed that explicitly models faulty sensors. Building on this approach, a novel algorithm has also been introduced to adaptively compensate faults leading to better traffic state estimation performance. The approach has been tested for freeway traffic density estimation in the context of the asymmetric cell transmission model and shown to exhibit robust and good quality state estimation performance that is very close to non-faulty estimation, irrespective of the fault magnitudes.

For future work we intend to examine the effect of model parameter changes and how such changes can be identified and estimated jointly with sensor faults. The efficiency of the approach will also be investigated for high-order macroscopic flow models that have nonlinear dynamics. Finally, the development of fast and efficient optimization algorithms for the introduced approaches will be examined to enable distributed, real-time, and large-scale estimation.

References

[1] S. Timotheou, C. G. Panayiotou, and M. M. Polycarpou, "Transportation systems: Monitoring, control, and security," in *Intelligent Monitoring, Control, and Security of Critical Infrastructure Systems*, pp. 125–166, Springer, 2015.

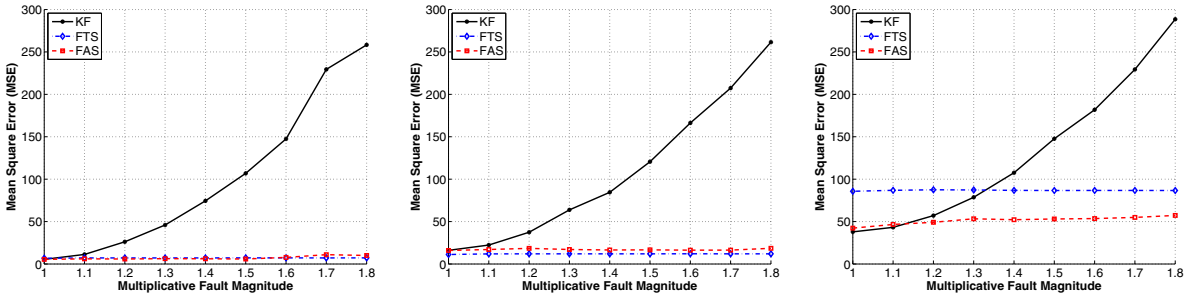

(a) (b) (c)

Fig. 2: TSE Mean Square Error of algorithms KF, FTS, and FAS for varying multiplicative magnitude error at ILD3 for measurement and process noise equal to: (a) $\mathbf{R} = \mathbf{I}$ and $\mathbf{Q} = \mathbf{I}$, (b) $\mathbf{R} = 9\mathbf{I}$ and $\mathbf{Q} = \mathbf{I}$, and (c) $\mathbf{R} = \mathbf{I}$ and $\mathbf{Q} = 9\mathbf{I}$.

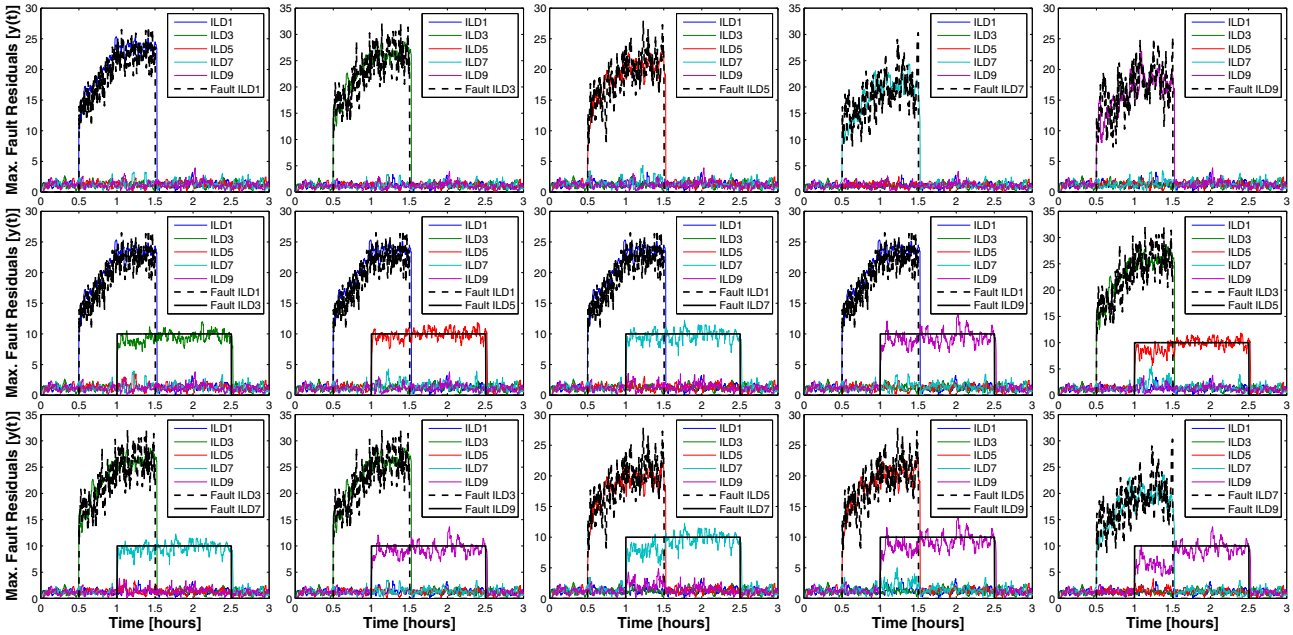

Fig. 4: Maximum fault residuals for all combinations of one and two faults(one additive and one multiplicative) at different ILDs.

[2] J. C. Herrera and A. M. Bayen, "Incorporation of Lagrangian measurements in freeway traffic state estimation," *Transportation Research Part B: Methodological*, vol. 44, no. 4, pp. 460–481, 2010.

[3] Y. Wang and M. Papageorgiou, "Real-time freeway traffic state estimation based on extended Kalman filter: a general approach," *Transportation Research Part B: Methodological*, vol. 39, no. 2, pp. 141–167, 2005.

[4] D. B. Work, S. Blandin, O.-P. Tossavainen, B. Piccoli, and A. M. Bayen, "A traffic model for velocity data assimilation," *Applied Mathematics Research eXpress*, vol. 2010, no. 1, pp. 1–35, 2010.

[5] L. Muñoz, X. Sun, R. Horowitz, and L. Alvarez, "Traffic density estimation with the cell transmission model," in *Proceedings of the 2003 American Control Conference*, vol. 5, pp. 3750–3755, 2003.

[6] C. Tampere and L. Immers, "An extended kalman filter application for traffic state estimation using ctm with implicit mode switching and dynamic parameters," in *Proceedings of the IEEE Intelligent Transportation Systems Conference (ITSC)*, pp. 209–216, Sept 2007.

[7] R. Rajagopal and P. P. Varaiya, *Health of California's Loop Detector Sytem*. California PATH Program, Institute of Transportation Studies, University of California at Berkeley, 2007.

[8] C. Chen, J. Kwon, J. Rice, A. Skabardonis, and P. Varaiya, "Detecting errors and imputing missing data for single-loop surveillance systems," *Transportation Research Record: Journal of the Transportation Research Board*, vol. 1855, no. 1, pp. 160–167, 2003.

[9] R. E. Turochy and B. L. Smith, "New procedure for detector data screening in traffic management systems," *Transportation Research Record: Journal of the Transportation Research Board*, vol. 1727, no. 1, pp. 127–131, 2000.

[10] S. Robinson and J. W. Polak, "Inductive loop detector data cleaning treatments and their effect on performance of urban link travel time models," in *Transportation Research Board 85th Annual Meeting*, no. 06-0989, 2006.

[11] H. J. Payne and S. Thompson, "Malfunction detection and data repair for induction-loop sensors using i-880 data base," *Transportation Research Record: Journal of the Transportation Research Board*, vol. 1570, no. 1, pp. 191–201, 1997.

[12] X.-Y. Lu, P. Varaiya, R. Horowitz, and J. Palen, "Faulty loop data analysis/correction and loop fault detection," in *Proceedings of the 15th World Congress on Intelligent Transport Systems*, 2008.

[13] J. Rawlings, "Moving horizon estimation," in *Encyclopedia of Systems and Control*, pp. 1–7, Springer, 2014.

[14] G. A. Terejanu, "Discrete kalman filter tutorial," *University at Buffalo, Dept. of Computer Science and Engineering*, vol. 14260, 2013.

[15] R. E. Kalman, "A new approach to linear filtering and prediction problems," *Journal of Fluids Engineering*, vol. 82, no. 1, pp. 35–45, 1960.

[16] A. Y. Aravkin, J. V. Burke, and G. Pillonetto, "Optimization viewpoint on kalman smoothing with applications to robust and sparse estimation," in *Compressed Sensing & Sparse Filtering*, pp. 237–280, Springer, 2014.

[17] E. Chu, A. Keshavarz, D. Gorinevsky, and S. Boyd, "Moving horizon estimation for staged QP problems," in *Proceeding of the IEEE 51st Annual Conf. on Decision and Control*, pp. 3177–3182, 2012.

[18] L. Munoz, X. Sun, D. Sun, G. Gomes, and R. Horowitz, "Methodological calibration of the cell transmission model," in *Proceedings of the 2004 American Control Conference*, vol. 1, pp. 798–803, 2004.

[19] V. Kekatos and G. B. Giannakis, "From sparse signals to sparse residuals for robust sensing," *IEEE Transactions on Signal Processing*, vol. 59, no. 7, pp. 3355–3368, 2011.